GCSM
11th Global Conference on Sustainable Manufacturing
2013
23rd - 25th September
Berlin - Germany

11.6 Optimization design of tandem blade rotor of new savonius hydrokinetics turbine model

B. Wahyudi [1], S. Soeparman [2] H.W.M. Hoeijmakers [3]
[1] Mechanical Engineering Department, State Polytechnic of Malang, Indonesia
[2] Mechanical Engineering Doctoral Program, Brawijaya University of Malang, Indonesia
[3] The Laboratory of Engineering Fluid Dynamics, University of Twente, Netherland

Abstract
The Fossil energy crisis prompted many studies to design energy conversion machines from renewable natural sources. One of them is the development of a model turbine savonius with tandem blades for hydropower. For the preliminary research, three model options of tandem blade savonius (TBS) were designed, i.e.: Overlap TBS, Symmetrical TBS, and Convergent TBS. This study aims to determine the best model and the optimal size of the tandem radius (Rt) and clearance blade (e) to produce a maximum pressure drop (ΔP). The method used is to apply CFD simulation and optimization using Response Surface Method (RSM). The best selection model and the result of the optimization design is convergent TBS model with Rt = 27 [mm] and e = 2.75 [mm] capable to generate maximum pressure drop ΔP = 9415.91 [Pa].
Keywords:
Tandem Blade; Savonius; Hydro-kinetic; RSM Optimization; CFD Simulation

1 INTRODUCTION

The effect of fast growing application of computational fluid dynamics (CFD) within the last two decades is the significance of numerical flow simulations in the design of hydraulic machinery that has grown to a considerable extent. At present, CFD simulations can often replace laboratory experiments due to the fact that even complex geometries and entire machines can be modeled. Many researches were conducted to demonstrate the influence of modified Savonius rotor blade geometry parameters such as twist blade, overlap ratio, amount of blade, multi-stage, sweep area, none circular blade, and additional guide blade on the aerodynamic performance of the rotor blade. However, the influence of geometrical design variables and their interactions on the rotor aerodynamic performance was not examined in detail in these works. From this point of view, the present research is focused on suggesting a rotor blade shape design using the numerical optimization method coupled with the statistical approach. Response surface method (RSM) is a collection of statistical and mathematical techniques useful for developing and improving the optimization process, which uses collectively design of experiment, regression analysis, and analysis of variance [1].

The Savonius hydrokinetic turbine is simple geometry and its construction is low-cost to manufacture. It starts rotating at lower speeds as compared to its counterpart hydraulic turbines, having a high starting torque. It produces low noise and can make use of the water river flowing in any horizontal direction to its rotation. However, in spite of these advantages, this turbine faces one main disadvantage of having low efficiency. The preliminary study has been done to choose the best design rotor tandem blade of savonius (TBS). By using the result CFD simulation of the three models i.e.: (a) Overlap TBS, (b) Symmetrically TBS and (c) Convergent TBS as shown in Fig. 1, 2 and 3, one of the best choice to be deeply studied is obtained. The optimum turbine power generation predicted by taking into calculation maximum pressure gap (Δ p) between upstream and downstream is Type Convergent TBS [2].

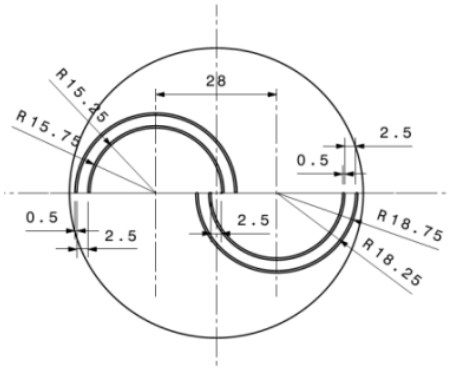

Figure 1: Overlap TBS (Type I)

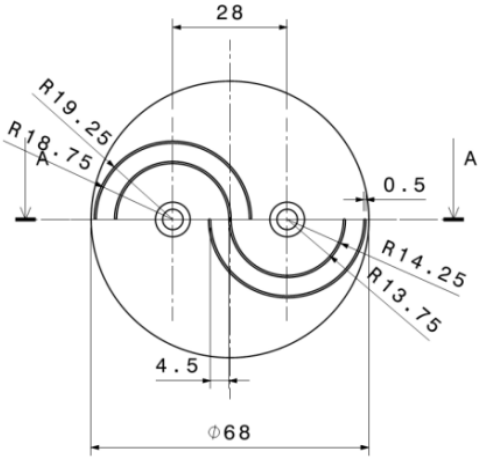

Figure 2: Symmetrically TBS (Type II)

G. Seliger (Ed.), Proceedings of the 11th Global Conference on Sustainable Manufacturing - Innovative Solutions
ISBN 978-3-7983-2609-5 © Universitätsverlag der TU Berlin 2013

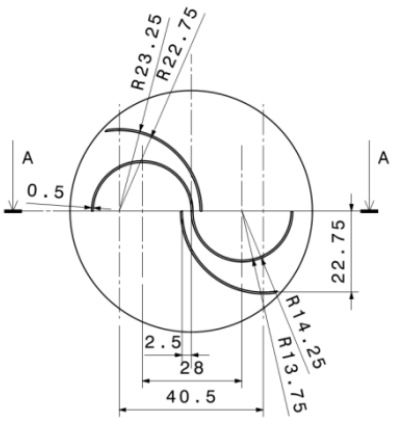

Figure 3: Convergent TBS (Type III)

The Savonious conventional has two pairs of cylindrical blade that look like a letter S which not connected to the middle or with gaps (overlapping) on both ends of the blade that serves as the entry of outflow from the first blade (thrust) to the second blade (return). As shown in Fig. 4, the first blade (advancing blade) got a drag force from the main flow (free flow) while the second blade (returning blade) got a returned force from the opposite direction outflow through the gap (overlap) resulting in a pair off couple force that is able to generate torque and power.

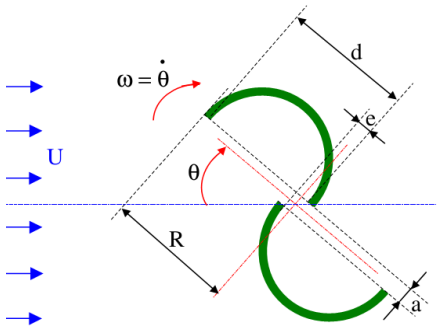

Figure 4: Original Savonius Rotor

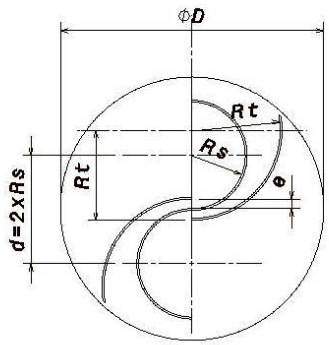

Figure 5: Convergent Tandem Blade Savonius

This paper focuses on optimization using RSM for designing geometry of Convergent TBS as shown in Fig.5 above. Objective of this study is to determine the value of the independent variables that cause the value of maximum pressure gap between upstream and downstream to be optimal. In these experiments, the response variable pressure gap (y) is affected by two independent variables: Radius Tandem Blade " *Rt* " or (x_1) and Clearance Blade "*e*" or (x_2). By using an appropriate model formulation, the value of independent variables (x_1, x_2) which causes maximum pressure gap designation optimal can be obtained.

2. RESPONSE SURFACE METHOD (RSM)

To understand how far the optimum process is influenced by number of variables, it is often necessary for experimental data to be large and takes a long time, which automatically also cost a huge amount. Several statistical and mathematical techniques are often used to make an approach to gain understanding of the optimum conditions of the process or design without requiring too much data. Among the commonly used method is the response surface method (RSM).

RSM is a set of mathematical and statistical techniques that are useful for analyzing problems where several independent variables affect the response variable and the ultimate goal is to optimize the response. The basic idea of this method is the use of statistical experimental design assisted to find the optimal value of the response. This method was first proposed in 1951 and has been used extensively in both the research and industrial applications until today. For example, by constructing a mathematical model, researchers can determine the value of the independent variables that lead to an optimal value of the response variable.

The first step of the RSM is to find a relationship between the response variable y with xi independent through a first order polynomial equation (model order I). Independent variables denoted by x1, x2, ..., xk. These variables are assumed to be controlled by the researcher and the influence response variable y is assumed as a random variable. If the response is well modeled by a linear function of the independent variables xi, the function approximation of the model order I are:

$$y = \beta_0 + \sum_{i=1}^{k} \beta_i x_i + \varepsilon \qquad (1)$$

with, y : dependent variable (response)
xi : factors that influence response variables, i = 1, 2, k
ε : residual component (error) which is random and distributed identical and independent (Independent Identically Distributed-IID) Normal distribution with the average value of 0 and variance σ2. In mathematically expressed by $\varepsilon \approx$ IID Normal $(0, \sigma^2)$.

Furthermore, at the condition near the response, the second order model (order II) or more normally required to approximate the response due to the curvature in the surface. In many cases, the model order II two expressed in equation (2) is considered sufficient.

$$\hat{y} = \beta_0 + \sum_{i=1}^{k} \beta_i x_i + \sum_{i=1}^{k} \beta_{ii} x_i^2 + \sum_{i} \sum_{j} \beta_{ij} x_i x_j, i < j \qquad (2)$$

Analysis of the response surface fitting Order II is often referred as the canonical analysis [1]. Least squares method is used to estimate parameters on the approximation functions. The subsequent RSM analysis can be used for surface fitting. If the surface fitting is a good approximation of a function of the response, surface fitting analysis would be equivalent with the actual analysis systems.

Analysis of variance and regression analysis are the statistical techniques to estimate regression coefficients in the quadratic

polynomial model and also yield a measure of uncertainty in the coefficients. One of the important statistical parameters is the coefficient of determination, R^2 which provides the summary statistic that measures how well the regression equation fits the data. It is given as:

$$R^2 = \frac{SSR}{SSTO} = 1 - \frac{SSE}{SSTO} \quad (3)$$

where SSTO is the total sum of squares, SSR is the regression sum of squares, and SSE is the error sum of squares. From the inspection of Equation (3), it is found that $0 \leq R^2 \geq 1$. However, a large value of R^2 does not necessarily imply that the regression model is a good one. Adding a variable to the model always increases R^2, regardless of whether the additional variable is statistically significant or not. Thus, it is possible for the models that have large values of R^2 to yield the poor predictions of new observations or estimates of the mean response. Because R^2 always increases as we add terms to the model, the adjusted -R^2 statistic parameter, R^2adj defined below is frequently used.

$$R^2_{adj} = 1 - \frac{SSE/(n_s - n_{rc})}{SSTO/(n_s - 1)} = 1 - \left(\frac{n_s - 1}{n_s - n_{rc}}\right)(1 - R^2) \quad (4)$$

In general, the adjusted-R^2 statistic does not always increase as variables are added to the model. In fact, if unnecessary terms are added, the value of R^2 *adj* often decreases.

It is important to determine the value of each regression variable in the regression model, because the model may be effective with the inclusion of additional variables or with the deletion of the variables already in the model. The test statistic (t-statistic) for testing the significance of any individual regression coefficient is

$$t = \frac{c_j}{\sqrt{\sigma^2 C_{jj}}}, \qquad j = i, \ldots \ldots, n_{rc} \quad (5)$$

Where σ^2 is the estimation of variance and C_{jj} is the diagonal element of $(X^TX)^{-1}$ corresponding to c_j.

3. DEVELOPMENT OF SAVONIUS ROTOR

Currently, the Savonious turbine has been developed with various modifications with the purpose of improving their performances. Cesar Humberto [3] combined the simulation and optimization method using genetic algorithm (GA) to design modified savonius rotor. Browsing point of optimization by using Polar Coordinate system for changing the shape of original rotor savonius combining with Banesh rotor produce a new shape of rotor savonius which is more efficient.

Menet, J .[4] has modified the savonius rotor which only changes the position of an off-set the second pair of rotor blades, now has three geometric parameters, namely: (1) primary overlap (e), secondary overlap (e '), and the angle between the axis blades (β). The result is relatively expected s new rotor induces maximum value of static torque is much higher than those obtained with the conventional rotor. However, they found low values and negative torque when an angle β has large variations. Overall, the average value of the torque increased to Cm = 0.48 or 60% more than the conventional rotor.

Fujisawa and Gotoh [5] has published a study comparing experimental results with a numerical study also using the discrete vortex method. He concluded that the numerical calculations were adequate to "predict the basic features of the variation in flow fields with rotor angle". Nevertheless, the procreation of the flow field around a stationary rotor was poor, and Fujisawa supposed that it was due to false assumptions used in the calculations. Sometimes, some visualizations of the flow in and around the rotor are proposed, but with a poor description of the physical phenomena. Fujisawa [6] also presented a exclusive description of the Visualization study of the flow in and around a of the conventional Savonius rotor, they conclude that the overall pressure coefficient decreased due to the effect of the circulation generated by rotor rotation. This is a phenomenon of circulation persists in revolving condition compared with stationary rotor, where the flow through the overlap is reduced due to backflow. The flow is expected to reduce the effect of pressure recovery on the back side of blade behind because of the pressure distribution near the overlap.

Kamoji et al. [7] improved the coefficient of power and obtained uniform coefficient of static torque. To achieve these objectives, the rotors are being studied with and without central shaft between the end plates. Experimental tests in a closed jet wind tunnel on modified form of the conventional Savonius rotor with the central shaft have the value of Cp = 0.32. They studied the effect of geometrical parameters on the performance of the rotors in terms of coefficient of static torque, coefficient of torque and coefficient of power. The parameters studied are overlap ratio, blade arc angle, aspect ratio, and Reynolds number.

Performance of Savonious hydro-kinetic turbine has dependence with the principle to generate drag forces is formulated by F = ½. ρ. A.U^2, thus optimizing torque and power turbine formation is highly dependent on the blades swept area (A) and velocity of fluid (U). Therefore, this paper introduced a new concept design of Savonius rotor by broadening swept area of tandem blade that can increase drag force production on the blade as shown as Fig. 3. To achieve the maximum power generation using convergent TBS rotor design, we use CFD simulation and RSM to realize optimum Radius Tandem Blade (Rt) and Clearance Blade (e) as independence variable.

4. CFD SIMULATION

By adapting the law of Navier-Stokes model of rotation frame, the equations governing the behavior Savonious hydrokinetics turbines will be used in this study. The equations rule the behavior of fluid flow including conservation of mass (eq. 6) and momentum equations (eq. 7). Two types of acceleration in the momentum equation representing two Savonious hydrokinetics turbine rotation are the Coriolis acceleration, (2 ω̃ x ῡr) and the centripetal acceleration (ω̃ x ω̃ x r̃).

$$\frac{\partial \rho}{\partial t} + \nabla . \rho \bar{\upsilon}_r = 0 \quad (6)$$

$$\frac{\partial}{\partial t}(\rho \bar{\upsilon}_r) + \nabla . (\rho \bar{\upsilon}_r . \bar{\upsilon}_r) + \rho(2\tilde{\omega} \times \bar{\upsilon}_r + \tilde{\omega} \times \tilde{\omega} \times \tilde{r}) = -\nabla p + \nabla \tau + F \quad (7)$$

In this equation, r̃ is the radial position of the rotating domain forms, ω̃ domain is the angular velocity of the rotor, $\bar{\upsilon}_r$ is the relative velocity, p is the static pressure, τ is the stress tensor and F represents the external body force. Adopting a combined formulation in cylindrical coordinates and Cartesian, in order to simulate two separate regions of the domain, i.e. inflows rotate the rotor-stator and external. Standard K-ε model, Eq. (8) and (9), is used to simulate the turbulence in the flow field [8]. They are coupled to the Navier-Stokes equations although included in the convection zone. It is a widely used and provides sufficient accuracy and worthy to represent the various types of flow. K-ε model is a two-equation models involving turbulent kinetic energy, k, and the dissipation rate, ε, as follows,

$$\frac{\partial}{\partial t}(\rho k) + \frac{\partial}{\partial x_i}(\rho k u_i) =$$

$$\frac{\partial}{\partial x_j}\left[\left(\mu+\frac{\mu_t}{\sigma_k}\right)\frac{\partial k}{\partial x_j}\right]+G_k+G_b-\rho\varepsilon-Y_M+S_k \quad (8)$$

$$\frac{\partial}{\partial t}(\rho\varepsilon)+\frac{\partial}{\partial x_i}(\rho\varepsilon u_i)=\frac{\partial}{\partial x_j}\left[\left(\mu+\frac{\mu_t}{\sigma_\varepsilon}\right)\frac{\partial \varepsilon}{\partial x_j}\right]+C_{1\varepsilon}\frac{\varepsilon}{k}(G_K+C_{3\varepsilon}G_b)-C_{2\varepsilon}\rho\frac{\varepsilon^2}{k}+S_\varepsilon \quad (9)$$

$$\mu_t=\rho\,C_\mu\,\frac{k^2}{\varepsilon} \quad (10)$$

In this model, G_k represents the generation of turbulence kinetic energy due to the velocity gradient, whereas G_b describe the generation of turbulence kinetic energy due to buoyancy, and Y_M is the contribution of the fluctuating dilatation to the overall dissipation rate. Variable σ_k and σ_ε are Prandtl numbers for the turbulent with value of k = 1.0 and ε = 1.3. Constants $C_{1\varepsilon}$ = 1.44 and $C_{2\varepsilon}$ = 1.92. Turbulent viscosity (or Eddy current), μ_t is computed by combining k and ε as shown in Eq. 10, where Cμ = 0.09.

This equation will be used to predict fluid flow through a turbine that will improve its performance.

By using simulation software ANSYS Release 14.5 it's the following boundary conditions that have been applied. The stationary domain has a free stream velocity. The hydrodynamic pressure conditions are applied and the initialization is done. Inlet and Outlet are default boundary conditions in simulation software. Inlet requires the speed of inlet velocity of water and the outlet requires the relative pressure, 1.0132 x 105 [Pa], at the initial conditions. The blade surfaces are enabled a "wall" condition. This condition enables the calculation of properties such as force, torque on the surface. Once the domains have been specified, a default fluid-fluid interface is detected between the rotating and stationary domain.

A two-dimensional view of the rotor model was considered. It is because the rotor blades rotate in the same plane as the approaching water flow stream. The computational domain was discretisized using two-dimensional unstructured mesh (triangular mesh). The left boundary had Velocity Inlet condition while the right boundary had Outflow condition. The top and bottom boundaries for the open channel sidewalls had symmetry conditions. The moving wall condition was employed for the rotor model to study the effect of fluid motion in and around the rotating Savonius rotor. The dimensions of the computational domain were 500 mm in length and 75,5 [mm] in width, which were also similar to the experimental conditions. For the various model conditions, the geometry of the rotor was changed and accordingly different meshes were generated for each condition.

Steps in the simulation solutions consist of:

1. Solver (Pressure Based, Steady, 2D)
2. Viscous Model: Standard k-epsilon (k-ε) / Near-Wall Treatment: Standard Wall Functions
3. Material: Water (μ = 1.002x10-3 [kg/m-s], ρ= 1.000 [kg/m3])
4. Operating conditions: Atmospheric Pressure (1.0132 [bar])
5. Boundary Conditions:
   - Inlet: Velocity Inlet
   - Sides: No slip wall
   - Blades: Stationary Wall
   - Outlet: Outlet
6. Solution controls:
   - Pressure Velocity Coupling: SIMPLE
   - Discretization: fluids
7. Pressure (Standard) / Inlet Velocity: 1 [m/s]

5. RESULT AND DISCUSSION

In the contour plots as shown at Figure 5, the blade on the left hand side is the returning blade and that on the right hand side is the advancing blade. The contour plots predict the variations in velocity and pressure in various regions near the blades within the flow domain. It can be observed from the pressure contour plots that pressure gap occur across the rotor from upstream to downstream side. This pressure gap indicates power extracted by the rotor causing its rotation [5]. The static pressure on the convex side of both the blades can be observed to be lower than those on the concave side of the blades; in fact, a region of negative pressure exists on the convex side of the blades. This occurs due to the high flow velocity over the convex side of the blades. As a result, a pressure difference acts across the concave and convex side of the blades, which provide the necessary torque for causing rotation of the blades.

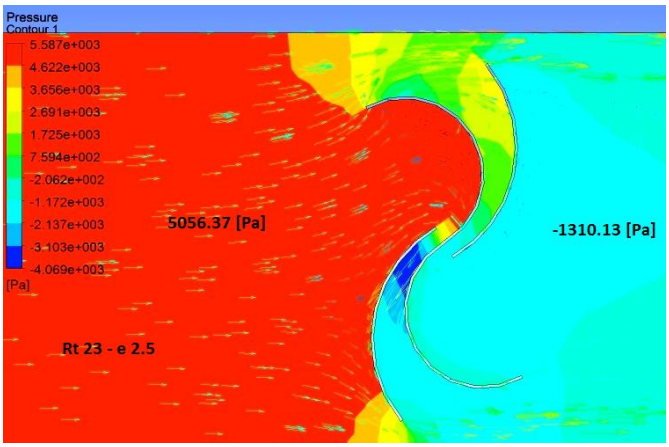

Figure 6: CFD simulation demonstrate the effect of Rt = 23[mm] and e = 2.5[mm] caused Δ P = 6366.5 [Pa]

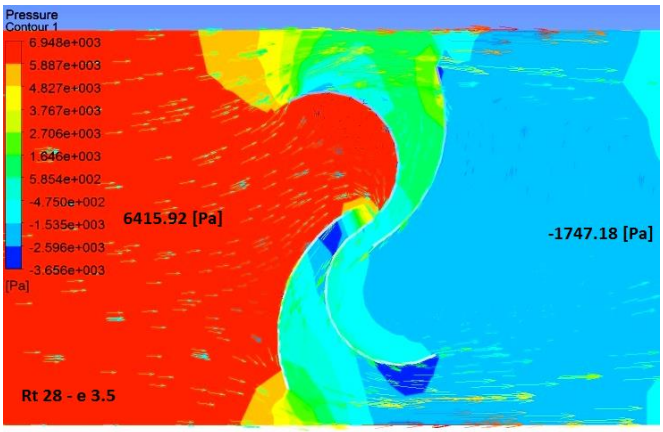

Figure 7: CFD simulation demonstrate the effect of Rt = 28 [mm] and e = 32.5 [mm] caused Δ P = 8163.1 [Pa]

Table 1: Central Composite Design Using Minitab R 14

Run Order	PtType	Blocks	Rt (mm)	e (mm)	ΔP (Pa)

1	1	1	23.0000	2.50000	6366.50
2	1	1	28.0000	2.50000	9134.91
3	1	1	23.0000	3.50000	5265.32
4	1	1	28.0000	3.50000	8163.10
5	-1	1	21.9645	3.00000	5039.54
6	-1	1	29.0355	3.00000	8817.03
7	-1	1	25.5000	2.29289	8721.59
8	-1	1	25.5000	3.70711	8835.92
9	0	1	25.5000	3.00000	8951.22
10	0	1	25.5000	3.00000	8951.22
11	0	1	25.5000	3.00000	8951.22
12	0	1	25.5000	3.00000	8951.22
13	0	1	25.5000	3.00000	8951.22

Table 2: Regression Coefficient Order II

Term	Coef.	SE Coef.	T	P
Constant	8951.2	187.9	47.626	0.000
RADIUS TANDEM BLADE	1376.0	148.6	9.261	0.000
CLEARANCE	-238.9	148.6	-1.608	0.147
RTB*RTB	-1166.7	159.3	-7.322	0.000
CLEARANCE*CLEARANCE	-241.5	159.3	-1.516	0.168

S = 420.3 R-Sq. = 94.7% R-Sq.(adj.) = 92.0%

To discuss the results of RSM optimization, as shown in Table 1 presented the CFD simulation data of rotor convergent TBS model using variable tandem radius (Rt) and Blade Clearance (e) with the lowest value of 23 mm - 2.5 mm and the highest 28 mm - 3.5 mm, both pressure gap indicates that each Δp = 6366.5 (Pa) and Δ p = 8163.1 (Pa). The two independent variables were considered as variables that affect maximize pressure gap (y), i.e., Radius (x_1) and Clearance (x_2). Experimental design used in the DoE is three-level factorial design (3k) using the Central Composite Design (CCD). The first step has been tested using a linear regression equation (Order I) with obtained R-square is only 54% and a P-value> 0.05 so it does not show any significance of the model.

Furthermore, similar test attempted to Order II model equations (linear + square) obtained a significant regression coefficient. To check the significance of the second-order model, it can be seen that p-value = 0.000 is less than the significance level α = 5%, see also that the independent variables x_1 made a significant contribution in the model, but x_2 is not significant. But, Overall this model it is able to demonstrate the high value of R-square = 94.7 % in Table 2, which means that the regression equation model is consistent with the real condition of the model studied. The model regression equation (11) is expressed:

$$\Delta P = 8951.2 + 1376\,(Rt) - 238.9\,(e) - 1166.7\,(Rt)^2 - 241.5\,(e)^2 + \varepsilon$$

After the optimization model has determined, the next step is to determine the conditions optimum of significant factors. From the contour plot of the image below, it can be concluded that the image does not have a stationary point. Consequently that calculation of the stationary point and surface characteristics of the response is not necessary. The result of response (ΔP) optimization will be obtained after value of (Rt) and (e) which substituted into the model equation above with constant value of Rt = 27 [mm] and variable e = 2.5 [mm] ÷ 3.5 [mm]. By using Minitab Software, it is more simple to obtain the result of peak point in the curvature as shown in Fig. 8 which show optimal value of Rt = 27 [mm] and e = 2.75 [mm] with response of maximum ΔP = 9415.91 [Pa].

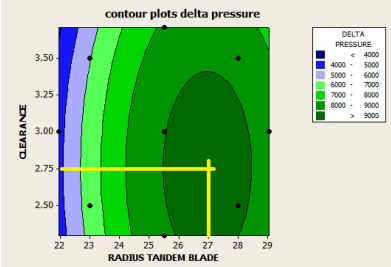

Figure 8: Contour Plot

6. CONCLUSION

Finally, with applied CFD simulation and optimization using RSM, we are able to assist design engineering of the critical part of convergent tandem blade of Savonius rotor that capable to generate maximum power on hydrokinetic turbine model. The result of design optimization of Savonius tandem blade is showed in Fig. 9 below with Rt = 27 [mm] and e = 2.75 [mm]. By using an appropriate model formulation eq. 11, the result value of independent variables "Rt" and "e" which causes maximum pressure gap designation optimal can be obtained which would be produce power maximum.

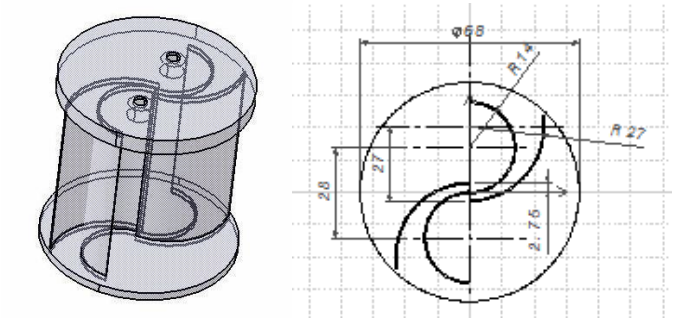

Figure 9: The result design of convergent TBS Rotor

7. REFERENCES

[1] Montgomery, D. C., 1984, Design and Analysis of Experiments, John Wiley & Sons, Canada.

[2] Bagus Wahyudi, et al., 2013, A Simulation Study of Flow and Pressure Distribution Patterns in and around of Tandem Blade Rotor of Savonius (TBS) Hydrokinetic Turbine Model, Journal of Clean Energy Technologies, Vol. 1, No. 4, July, p.p. : 286-291.

[3] Cesar Humberto, 2008, Optimization of the efficiency of a Savonius wind turbine for urban media using Genetic Algorithm, Master Thesis, Instituto Technologico De Monterrey.

[4] Menet, J, 2004, Increase in the Savonius Rotors Efficiency via a Parametric Investigation,. Available on http://www.2004ewec.info/files/23_1400_jeanlucmenet_01.pdf

[5] N . Fujisawa and F. Gotoh, 1992, Visualization study of the flow in and around a Savonius rotor, Exp. in Fluids,12(6), pp. 407-412

[6] N. Fujisawa, 1996, Velocity measurements and numerical calculations of flow fields in and around Savonius rotors.' J. Wind Eng. Ind. Aero.; 59 , pp.: 39-50.

[7] M.A. Kamoji, S.B. Kedare, S.V. Prabhu, 2009, Experimental investigations on single stage modified Savonius rotor, Applied Energy, vol. 86, no. 7-8 pp.: 1064-1073.

[8] Pope Kevin, 2009, Performance Assesment of Transient Behaviour of Small Wind Turbines, Master Thesis in Applied Science, University of Ontario Institute of Technology.